

MIXED SENSITIVITY CONTROL DESIGN AND STABILITY ANALYSIS OF BRUSHLESS DOUBLY FED INDUCTION GENERATOR

A. GANOUCHE H. BOUZEKRI A. BEDDAR

Automatic Laboratory of Skikda, University 20 August 1955 Skikda, Algeria

B.P.26 route d'El-Hadaiek, 21000, Algeria, Skikda,

ganouche.a@gmail.com, habouzekri@gmail.com, antar_tech@hotmail.fr

Abstract: *The brushless doubly-fed induction machine continues to attract increasing interest for applications in wind power generation systems and variable speed motor drives where, robustness and low servicing costs are much desirable. This paper presents an H_∞ control of a grid connected variable speed wind energy conversion system based brushless doubly-fed induction machine. For this purpose, a linearized small signals mathematical model has been developed, and the mixed sensitivity control theory has been used. To enhance the performances of the mixed sensitivity design, decoupling and integral actions have been considered. Additionally, the effect of electrical parameters uncertainties and operating speed change on the stability of the brushless doubly-fed induction machine has been given. The proposed control scheme has been investigated through simulation implementation under different modes of operation, sub-synchronous, synchronous and super-synchronous mode. The obtained results show that the controller provides satisfying performances when the operating point varies.*

Key words: *brushless doubly fed induction machine, small signal model, stability analysis, parameter variation, mixed sensitivity, robustness.*

1. Introduction.

The Brushless Doubly Fed Induction Machine (BDFIM) has emerged as a promising alternative in wind energy conversion system to overcome the drawbacks of the Doubly Fed Induction Generator (DFIG) which requires periodic servicing, thus inducing extra maintenance costs [1].

The first literature reports on the BDFIM structure can be traced back to the early years of the twentieth century when Hunt [2] proposed a topology based on two DFIGs rotating on the same shaft with their rotor windings connected to form what was known as the 'cascaded DFIGs'. This structure was further improved by allowing a special single rotor to couple two independent three-phase windings known as Power Winding (PW) and Control Winding (CW) located on the stator. The stator windings (PW and CW) are designed with different pole pair numbers to eliminate direct magnetic coupling [3-4]. In generation mode, the PW is connected directly to the grid and the CW is fed by a back-to-back converter [5]. To obtain synchronous

operation of the BDFIM, an electromagnetic cross-coupling effect between the PW and CW must be achieved such that the induced rotor currents evolve with equal frequencies [6].

Recently, many mathematical models have been proposed to describe the steady-state and the dynamic behaviour of the BDFIM for exploitation in implementing control strategies and studying its stability [1, 5-8].

In the reported literature, many control strategies have been proposed to control the BDFIM such as the optimal sensorless control [9], the sliding mode control [10-12], the fuzzy control [13] and the adaptive control [14]. In the previous published work, no robust control is proposed due to the lack of a clear mathematical model of the BDFIM.

A few robust control attempts of the BDFIM have been carried out. In [15] a H_∞ mixed sensitivity control has been proposed on a second order BDFIM reduced model. Later on, using the same model, [16] proposed the adoption of L_2 robust control method in order to perform a controller which can guarantee that the turbine meets required performances under parameters uncertainties.

This paper presents a robust control applying H_∞ mixed sensitivity for a BDFIM in wind generation. The generator is considered directly connected to the grid. The transfer matrix model of the grid-connected-BDFIM is developed from the existing time varying vector model by using the small signal approach. In order to ameliorate the performances of the H_∞ mixed sensitivity, a decoupling matrix term has been used, and an integral action has been introduced. In addition to the proposed control scheme, eigenvalues techniques were employed to analyse the stability characteristics of the BDFIM for different equilibrium points and under parameters change.

The rest of the paper is organized as follows. In Section 2 the small signal unified reference frame model of the BDFIM in wind energy system is derived.

Section 3 presents a stability study based on the proposed model and applied to a selected benchmark machine. Section 4 presents the proposed control scheme for a BDFIM. Finally, conclusions are drawn in section 5.

2. Mathematical model of the BDFIM

The principle of using a grid-connected BDFIM in generation mode in a wind energy conversion system is illustrated in Fig.1. In this variable speed structure, the CW is connected to the grid through a partially rated power electronic converter.

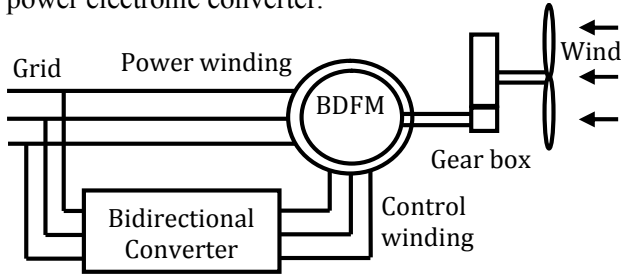


Fig. 1. The BDFIM in wind energy conversion system.

Based on the set of electromagnetic equations of the BDFIM expressed in the a-b-c coordinate system, the machine model aligned with the PW flux and expressed in the dq unified reference frame is given by the following expressions [8]:

The voltage equations are:

$$v_{dqp} = R_{sp}i_{dqp} + \frac{d}{dt}\phi_{dqp} + j\omega_p\phi_{dqp} \quad (1)$$

$$v_{dq c} = R_{sc}i_{dq c} + \frac{d}{dt}\phi_{dq c} + j\alpha\phi_{dq c} \quad (2)$$

$$v_{dqr} = R_r i_{dqr} + \frac{d}{dt}\phi_{dqr} + j\beta\phi_{dqr} \quad (3)$$

The magnetic flux equations are:

$$\phi_{dqp} = L_{sp}i_{dqp} + L_{hp}i_{dqr} \quad (4)$$

$$\phi_{dq c} = L_{sc}i_{dq c} + L_{hc}i_{dqr} \quad (5)$$

$$\phi_{dqr} = L_r i_{dqr} + L_{hp}i_{dqp} + L_{hc}i_{dq c} \quad (6)$$

With:

$$\alpha = \omega_p - (p_p + p_c)\omega_r \quad (7)$$

$$\beta = \omega_p - p_p\omega_r \quad (8)$$

In the previous equations, v , i and ϕ represent voltage, current and flux quantities respectively, R for resistances, L_s and L_h are for self and mutual inductances respectively, ω_p is the supply frequency of the PW, ω_r is the rotor speed, p_p and p_c are the pole-pair numbers of PW and CW respectively, subscripts p , c and r mean PW, CW and rotor

respectively, subscripts d and q are for direct and quadrature axis of the dq reference frame. α is the relative angular velocity between the reference dq and the stator CW reference related to a p_c type distribution, and β is the relative angular velocity between the reference dq and the stator PW reference related to a p_p type distribution [8, 17].

Substitution of the flux Eqs. (4) to (6) into the Voltage Eqs. (1) to (3) yields:

$$\begin{bmatrix} v_{dp} \\ v_{qp} \end{bmatrix} = \begin{bmatrix} R_{sp} + qL_{sp} & -\omega_p L_{sp} \\ \omega_p L_{sp} & R_{sp} + qL_{sp} \end{bmatrix} \begin{bmatrix} i_{dp} \\ i_{qp} \end{bmatrix} \quad (9)$$

$$+ \begin{bmatrix} qL_{hp} & -\omega_p L_{hp} \\ \omega_p L_{hp} & qL_{hp} \end{bmatrix} \begin{bmatrix} i_{dr} \\ i_{qr} \end{bmatrix}$$

$$\begin{bmatrix} v_{dc} \\ v_{qc} \end{bmatrix} = \begin{bmatrix} R_{sc} + qL_{sc} & -\alpha L_{sc} \\ \alpha L_{sc} & R_{sc} + qL_{sc} \end{bmatrix} \begin{bmatrix} i_{dc} \\ i_{qc} \end{bmatrix} \quad (10)$$

$$+ \begin{bmatrix} qL_{hc} & -\alpha L_{hc} \\ \alpha L_{hc} & qL_{hc} \end{bmatrix} \begin{bmatrix} i_{dr} \\ i_{qr} \end{bmatrix}$$

$$\begin{bmatrix} v_{dr} \\ v_{qr} \end{bmatrix} = \begin{bmatrix} R_r + qL_r & -\beta L_r \\ \beta L_r & R_r + qL_r \end{bmatrix} \begin{bmatrix} i_{dr} \\ i_{qr} \end{bmatrix} \quad (11)$$

$$+ \begin{bmatrix} qL_{hp} & -\beta L_{hp} \\ \beta L_{hp} & qL_{hp} \end{bmatrix} \begin{bmatrix} i_{dp} \\ i_{qp} \end{bmatrix} + \begin{bmatrix} qL_{hc} & -\beta L_{hc} \\ \beta L_{hc} & qL_{hc} \end{bmatrix} \begin{bmatrix} i_{dc} \\ i_{qc} \end{bmatrix}$$

Where q represents the time derivative, $q = \frac{d(\bullet)}{dt}$.

Given the nonlinearities inherent to the previous model represented by Eqs. (9) to (11), a simplification can be justified under the assumption of small variations in the rotor's mechanical angular speed. Thus, for the case of a wind energy conversion system operating around an angular speed value ω_{ro} which depends on the wind nominal speed ($\omega_r = \omega_{ro} + \Delta\omega_r, \Delta\omega_r \approx 0$), Eqs. (7) and (8) become:

$$\alpha = \omega_p - (p_p + p_c)\omega_{ro} \quad (12)$$

$$\beta = (\omega_p - p_p\omega_{ro}) \quad (13)$$

Where the new subscript o denotes the steady state quantities.

In the sequel, it is assumed that the PW voltages are maintained constant. This assumption is particularly true for a machine connected to the grid and operating as a generator. In such a case, variations around the quiescent values of the PW voltages are neglected ($\Delta v_{dp} \approx 0$, $\Delta v_{qp} \approx 0$).

Now, combining Eqs. (9) (10) and (11) allows

expression of the PW current vector as a linear function of the CW voltage vector as follows [5]:

$$\begin{bmatrix} \Delta I_{dp}(s) \\ \Delta I_{qp}(s) \end{bmatrix} = [\mathbf{G}(s)] \begin{bmatrix} \Delta V_{dc}(s) \\ \Delta V_{qc}(s) \end{bmatrix} \quad (14)$$

Where $[\mathbf{G}(s)]$ is a 2x2 transfer function matrix defining the BDFIM as a two-input-two-output linear system with the following structure [5]:

$$[\mathbf{G}(s)] = \begin{bmatrix} G_{11}(s) & G_{12}(s) \\ -G_{12}(s) & G_{11}(s) \end{bmatrix} \quad (15)$$

Entries $G_{11}(s)$ and $G_{12}(s)$ of the transfer matrix $[\mathbf{G}(s)]$ are functions of both the rotor's nominal operating mechanical angular speed ω_{ro} and the electrical parameters of the machine. $G_{11}(s)$ and $G_{12}(s)$ are given by:

$$G_{11}(s) = \frac{b_1(s)}{a(s)}, G_{12}(s) = \frac{b_2(s)}{a(s)} \quad (16)$$

Where $a(s)$, $b_1(s)$ and $b_2(s)$ are polynomials in the Laplace variable 's':

$$b_1(s) = b_{15} \cdot s^5 + b_{14} \cdot s^4 + b_{13} \cdot s^3 + b_{12} \cdot s^2 + b_{11} \cdot s^1 + b_{10} \quad (17)$$

$$b_2(s) = b_{24} \cdot s^4 + b_{23} \cdot s^3 + b_{22} \cdot s^2 + b_{21} \cdot s^1 + b_{20} \quad (18)$$

$$a(s) = s^6 + a_5 \cdot s^5 + a_4 \cdot s^4 + a_3 \cdot s^3 + a_2 \cdot s^2 + a_1 \cdot s^1 + a_0 \quad (19)$$

The bloc diagram of the BDFIM is illustrated by Fig. 2.

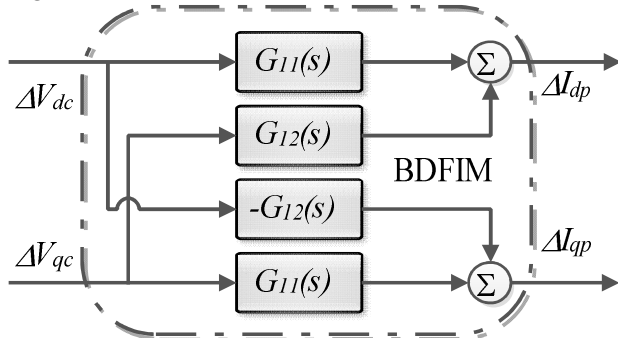


Fig. 2. BDFIM bloc diagram.

The linearized mathematical model of the BDFIM in Eq. (15) defines a multivariable linear structure in the s-domain which allows application of all tools and techniques made available by linear control theory for stability analysis and controller design of the machine.

Under synchronous conditions the two stator windings will co-operate to induce the same frequency and distribution of currents in the rotor cage and, the synchronous operation speed is equal to:

$$\omega_{sync} = \frac{\omega_p + \omega_c}{P_p + P_c} \quad (20)$$

In order to ensure that the BDFIM operate in the synchronous operation mode, the frequency of the CW must be:

$$\omega_c = (p_p + p_c)\omega_r - \omega_p \quad (21)$$

Note that the BDFIM model depends on the variable rotor's angular speed ω_{ro} on one hand and, on the less variable electrical parameters of the machine (resistances, self-inductances, coupling inductances) on the other hand.

3. Stability analysis of the BDFIM.

The stability of the BDFIM has been marginally studied. Cook et al. [18] studied the stability of a cascaded Doubly Fed Induction Machines (DFIM) mounted in a single frame by using small signal analysis; they concluded that the cascaded DFIM has some areas of instability in open loop operation. More recently, the same authors investigated the impact of parameters change on the stability of the cascaded DFIM and demonstrate that the real part of the dominant poles of the cascaded DFIM is dependent on the speed and load [19]. Li et al. [20] analyzed the open-loop stability characteristics of the BDFIM in equilibrium points based on the generalized theory of Floquet; they show by simulation results a possible instability when the frequency of the CW is high, but their experimental results disagree with those obtained by computer simulation, in fact, the BDFIM can achieve a full-speed range open-loop stable operation from no load to 50% loaded. [7, 21] studied the open-loop stability of a small signal dq unified reference frame model of the BDFIM, and show that the area of stability is dependent on machine parameters. Later on, [22] studied the stability of the BDFIM under closed loop scalar current control, and show by experimental BDFIM set-up a stable behaviour along all the operation range.

In the following, the proposed model is used to carry out a stability analysis of a selected benchmark BDFIM [17]. This machine has one pole pair in the PW, and three pole pair in the CW. The electrical parameters of the prototype are given in the Table 1.

Table 1

BDFIM electrical parameters

| | Resistance (Ω) | Self inductance (H) | Mutual inductance (H) |
|--------------------|----------------------------|---------------------------|-----------------------------|
| Power winding | 1.732 | 0.7184 | 0.2421 |
| Control winding | 1.079 | 0.1217 | 0.0598 |
| Rotor | 0.473 | 0.1326 | |

3.1. BDFIM stability analysis with respect to the operating speed change

The first step in the analysis process is the determination of the coefficients of the common denominator $a(s)$ of the $[G(s)]$ transfer matrix elements. The result of the calculation of the sixth order polynomial $a(s)$ for the selected BDFIM in terms of the rotor's nominal mechanical speed ω_{ro} is given by Eq. (22).

Given that some coefficients are functions of the operating velocity ω_{ro} , the positions in the complex domain of the solutions of the equation $a(s)=0$ evolve accordingly and, define six branches as illustrated by Fig. 3.

$$\begin{aligned}
 a(s) = & s^6 + 110.44937s^5 + 1581359.7\omega_{ro}^4 \\
 & + s^4(299909.75 - 3141.5926\omega_{ro} + 17\omega_{ro}^2) \\
 & + s^3(2.1845414 \times 10^7 - 212688.6\omega_{ro} + 1156.427\omega_{ro}^2) \\
 & + s^2 \left(\begin{aligned} & 2.9824929 \times 10^{10} - 6.254463 \times 10^8 \omega_{ro} \\ & + 4958656.8\omega_{ro}^2 - 12566.371\omega_{ro}^3 + 16\omega_{ro}^4 \end{aligned} \right) \\
 & + s \left(\begin{aligned} & 1.0798009 \times 10^{12} - 2.101283 \times 10^{10} \omega_{ro} \\ & + 1.5144057 \times 10^8 \omega_{ro}^2 - 296246.76\omega_{ro}^3 \\ & + 377.19309\omega_{ro}^4 \end{aligned} \right) \\
 & + 9.8358765 \times 10^{14} - 3.1040242 \times 10^{13} \omega_{ro} \\
 & + 3.2414085 \times 10^{11} \omega_{ro}^2 - 1.2443846 \times 10^9 \omega_{ro}^3
 \end{aligned} \quad (22)$$

Figure 3 shows the evolution of the six complex poles for a velocity varying from zero up to 1500 rpm (1500 rpm represents the double of the synchronous speed ω_{sync}). In fact, for all possible values of rotor's angular velocity, the real part of the poles is negative, which indicates stable open loop BDFIM regardless of the rotor's operating velocity.

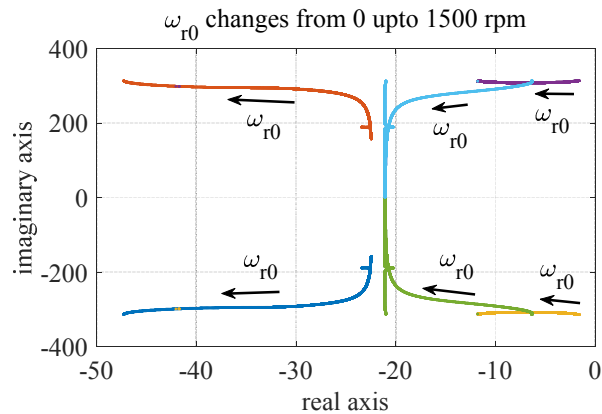


Fig. 3. Poles evolution w.r.t the operating velocity.

3.2. BDFIM stability analysis with respect to electrical parameters changes

Further simulations have been conducted to study the impact of changes in electrical parameters on the machine stability. Particular interest has been given on the effect of variations in rotor's resistance R_r and self-inductance L_r , as these parameters can undergo significant variations with rotor's temperature increase during machine operation [23-25]. The variation of a parameter x can be expressed as:

$$x = x_o \pm \Delta x \quad (23)$$

The relative uncertainty in percent can be written by:

$$\Delta x(\%) = \left(\frac{x}{x_o} - 1 \right) 100\% \quad (24)$$

Figure 4. and Fig. 5. represent the real part of the poles in function of variations in $\Delta R_r(\%)$ and $\Delta L_r(\%)$ respectively when the BDFIM turn at rated speed. Only $\pm 40\%$ of variation in parameters is taken into account. As can be seen, the stability of the BDFIM is not altered by any variations in R_r . However, if the stability is maintained for an increase of up to 40% in L_r , the BDFIM becomes open loop unstable for a decrease beyond 16% in the rotor self-inductance value.

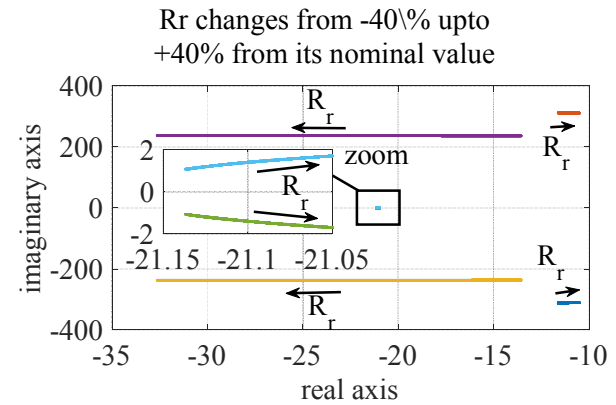


Fig. 4. Poles evolution with respect to rotor resistance variations.

An extensive simulation study has been done to evaluate the stability of the BDFIM when the electrical parameters seriously vary, as a result, the decrease in L_p by -20%, L_c by -30% or R_c by -40% from its normal value can destabilize the BDFIM. This decrease in electric parameters can be originated in most of the cases by some short-circuited turns in the coil.

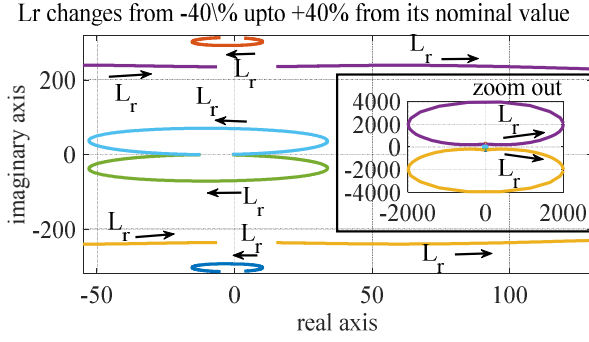


Fig. 5. Poles evolution with respect to rotor self-inductance variations.

4. BDFIM controller design

To control this machine, the following approaches have been adopted:

4.1. Decoupling matrix calculation

In order to facilitate the control scheme, and to avoid handling multi variable quantities, we propose the next decoupling operation.

To realize a perfect decoupling between the direct-axis components and the quadrature-axis components, the decoupling matrix must have the following form [26]:

$$H(s) = \begin{bmatrix} G_{11}(s) & -G_{12}(s) \\ G_{12}(s) & G_{11}(s) \end{bmatrix} \quad (25)$$

This is particularly harvestable in the case where the system to be controlled is an induction machine. In this case, the set BDFIM-Decoupling matrix is given by:

$$G(s)H(s) = \begin{bmatrix} \frac{b_1^2(s) + b_2^2(s)}{a^2(s)} & 0 \\ 0 & \frac{b_1^2(s) + b_2^2(s)}{a^2(s)} \end{bmatrix} \quad (26)$$

As we can see, the order of the obtained open loop system is twelve, and the transfer function between ΔV_{dc} and ΔI_{dp} is the same transfer function between ΔV_{qc} and ΔI_{qp} . Henceforth, we use the single-input-single-output notation rather than the old one MIMO notation.

4.2. H_∞ Mixed sensitivity control theory

The standard configuration of the H_∞ control problem is given by Fig. 6. [27-29]

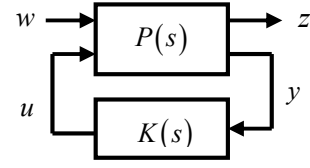


Fig. 6. General formulation of the H_∞ control problem

Where $P(s)$ represents the generalized plant, $K(s)$ the controller, w is the exogenous inputs, z denotes the output signals to be minimized, y is the measurement outputs and u is the control signals.

The interaction between inputs and outputs leads to a number of characteristic transfer matrices. We note particularly: the sensitivity function $S = (I + GK)^{-1}$, which represents the perturbation's influence on the measurement outputs; $R = K(I + GK)^{-1}$ which represents the impact of the perturbation on the control signals; the complementary sensitivity function $T = GK(I + GK)^{-1}$, which represents the influence of the measurement noise on the measurement outputs.

The analysis results prove that to obtain nominal performance and robust stability, the three matrices S , R and T have to be minimized. This synthesis may seem contradictory but it is not since these minimizations are imposed in different frequency ranges [30-33]. Henceforth, Weighting matrices $W_1(s)$, $W_2(s)$ and $W_3(s)$ are introduced and the above results are written in terms of three inequalities:

$$\|W_1 S\|_\infty < 1, \|W_2 R\|_\infty < 1, \|W_3 T\|_\infty < 1 \quad (27)$$

Or

$$\left\| \begin{bmatrix} W_1 S \\ W_2 R \\ W_3 T \end{bmatrix} \right\|_\infty < 1 \quad (28)$$

This result is known as the mixed sensitivity problem.

The H_∞ problem consists in minimizing the effect of perturbation on the system, i.e. minimizing the ratio $\left\| \frac{z}{w} \right\|_2$.

However, this ratio is equal, in the worst case to $\|F_1(P, K)\|_\infty$. F_1 is the lower Redheffer product.

The problem can be formulated as follows:

Given $P(s)$ and $\gamma > 0$, finding $K(s)$ which:

- stabilizes the closed loop system

- ensures $\|F_1(P, K)\|_\infty < \gamma$

Calculations prove that satisfying $\|F_1(P, K)\|_\infty < \gamma$

comes to satisfy $\frac{1}{\gamma} \left\| \frac{W_1 S}{W_2 R} \right\|_\infty < 1$ which is the condition

obtained in (28). The Mixed sensitivity structure is given on Fig. 7.

The good choice of weighting functions allowed us to perform good dynamic response with good robustness in stability.

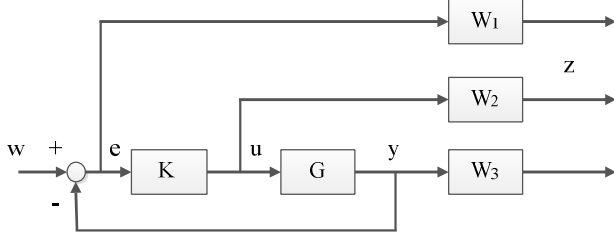


Fig. 7. Mixed sensitivity structure for H_∞ controller design.

The weighting functions chosen for our system which combines both the BDFIM model and the decoupling matrix are given by the method described in [34]:

$$W_1 = \frac{0.5(99.98 + s)}{0.04999 + s} \quad (29)$$

$$W_2 = 10^{-4} \quad (30)$$

$$W_3 = \frac{1000.(24.995 + s)}{49990 + s} \quad (31)$$

Unfortunately, the H_∞ mixed sensitivity regulator does not nullify the static error. The curve of singular values of $K(s)$ can easily reveal this problem, see Fig. 8.

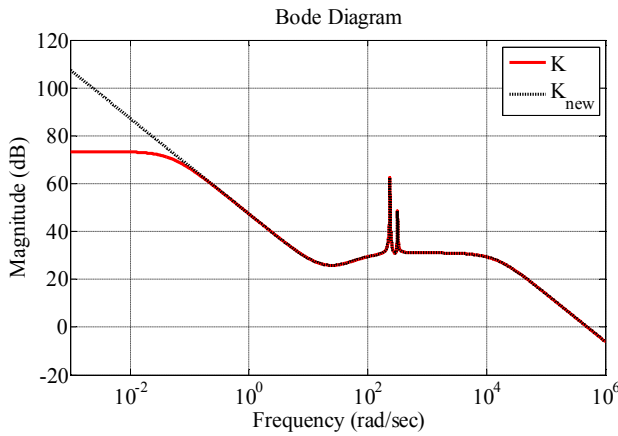


Fig. 8. Bode diagram of the regulator.

The static gain of the controller is very high, but not infinite. So, the regulator obtained does not cancel steady state error, but greatly decreases it. The regulator so has a pole close to the origin, but not exactly at the origin. To overcome this trouble, an integral action must be taken into account.

To incorporate and isolate a pure integrator, we can perform the partial fraction decomposition. We must locate the nearest pole to zero p_{k_i} (the dominant pole), find his residue k_i , and put the pole to zero.

$$K(s) = \frac{k_i}{s - p_{k_i}} + K_1(s) \quad (32)$$

The final controller is

$$K_{new}(s) = \frac{k_i}{s} + K_1(s) \quad (33)$$

The structure presented on Fig. 9. has been considered.

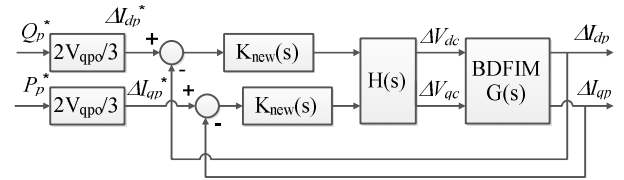


Fig. 9. Control diagram of the power winding currents.

The active power P_p and the reactive power Q_p of the PW are given by:

$$\begin{cases} P_p = \frac{3}{2}(v_{dp}i_{dp} + v_{qp}i_{qp}) \\ Q_p = \frac{3}{2}(v_{qp}i_{dp} - v_{dp}i_{qp}) \end{cases} \quad (34)$$

Given that the selected unified reference frame is aligned with the PW flux orientation. Therefore the direct component of the grid voltage is zero [9, 35]:

$$\begin{cases} v_{dp} = 0 \\ v_{qp} = v_p \end{cases} \quad (35)$$

Assuming that the grid voltage is maintained constant, the small signal relationship between the powers (active and reactive) of the PW and currents (direct and quadrature) of the PW can be written by:

$$\begin{cases} \Delta P_p = \frac{3}{2}(v_{qpo}\Delta i_{qp}) \\ \Delta Q_p = \frac{3}{2}(v_{qpo}\Delta i_{dp}) \end{cases} \quad (36)$$

Therefore, references of the PW currents can be obtained by:

$$\begin{cases} \Delta i_{qp}^* = \frac{2}{3 \cdot v_{qpo}} \Delta P_p^* \\ \Delta i_{dp}^* = \frac{2}{3 \cdot v_{qpo}} \Delta Q_p^* \end{cases} \quad (37)$$

In order to validate the proposed power control scheme of the BDFIM operating in generation mode for wind energy applications, a simulation is carried out using Matlab/Simulink. Results obtained for two different operating speeds are discussed hereafter.

Actually, the controller parameters were calculated for the synchronous speed. The BDFIM effective range is around $\pm 10\%$ of the synchronous speed. In order to evaluate the proposed controller outside the effective band, 650 (rpm) operating point have been chosen. It is important to note that when the rotor speed exceed its rated value, the pitch angle control intervene to make sure that the generated power is maximized. Accordingly, the super-synchronous mode will be not reachable.

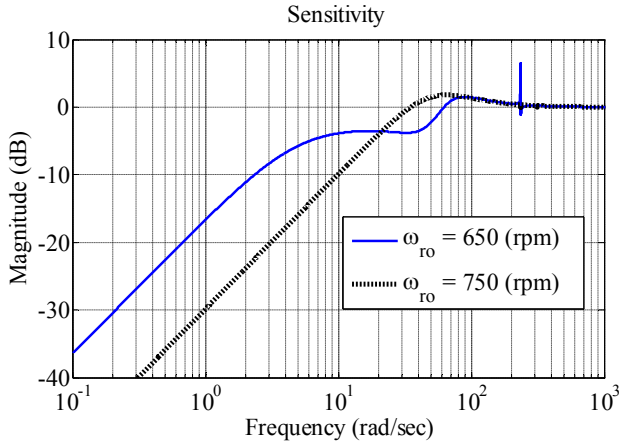


Fig. 10. Bode mag of the sensitivity function for two operating speeds.

Figure 10 represents the Bode magnitude (Singular values in the case of MIMO systems) of the sensitivity function for two different operating points. The solid curve is for $\omega_{r0} = 650(\text{rpm})$ and the dotted one is for $\omega_{r0} = 750(\text{rpm})$. The magnitude of the sensitivities is always less than or equal 6 (dB) whatever the frequency of the input signals, thus implies good margins of gain and phase. In the low frequencies, the magnitude of the sensitivities converge to $-\infty(\text{dB})$, thus indicate static error null. In the high frequencies, the sensitivities gain is held to zero, so we can conclude a good disturbance rejection. The bandwidth gives an idea about the settling time; therefore, the responses are expected to be fast.

The dynamic response of the system for a step of 2 (KW) in the active power, while the reactive power

reference is maintained to zero has been given for 750 (rpm) and 650 (rpm) in Fig. 11. and Fig. 12. respectively, assuming that the parameters are precisely identified.

As can be seen on Fig. 11. for the synchronous speed, the quadrature current of the PW represents a good track of its reference, with a good settling time, and without the overshoot. Additionally, the coupling effect between Δi_{dp} and Δi_{qp} i.e. active and reactive power is eliminated. For operating speeds other than the rated one (Fig. 12), the performances of the controller are slightly degraded with slower responses, but still remained better compared to those of the PI controller [5].

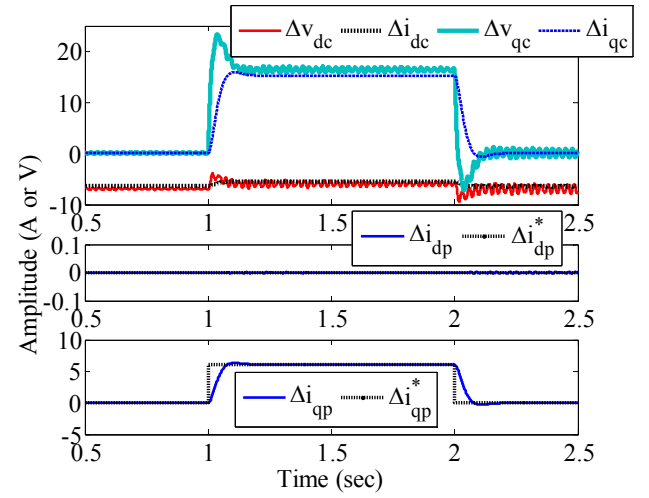


Fig. 11. Dynamic response when the rotor turns at rated speed without parameter uncertainties.

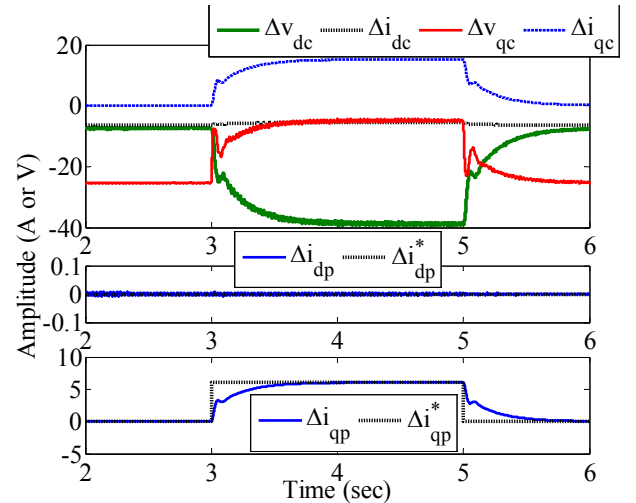


Fig. 12. Dynamic response when the rotor turns at 650 (rpm) without parameter uncertainties.

To present the main advantage of the obtained controller, we suppose that the electrical parameters of the BDFIM have been badly identified. To do so, we assume that the identified rotor parameters are

different by 5% from the real rotor parameters, and the identified stator parameters are different by 2% from the real stator parameters. The assumed real parameters of the BDFIM are given in Table 2.

Table 2

The assumed BDFIM real parameters

| | Resistance (Ω) | Self inductance (H) | Mutual inductance (H) |
|--------------------|----------------------------|---------------------------|-----------------------------|
| Power winding | 1.6974 | 0.7005 | 0.2373 |
| Control winding | 1.1006 | 0.1241 | 0.0610 |
| Rotor | 0.4493 | 0.126 | |

The dynamic response for a step of 2 (KW) in the active power, meanwhile the reactive power is regulated to zero is given by Fig. 13. for the synchronous operating speed, and by Fig. 14. for 650 (rpm) operating speed. As can be seen, the collected curves show comparable performances in the response time, the overshoot and the tracking error. In spite of the inaccurate electrical parameters used for the calculation of the controller, the dynamic responses are good as good as the case of precise parameters.

Regrettably, the change between the real parameters of the BDFIM and the identified ones leads to an imperfect decoupling between the d-axis and the q-axis, i.e. between the active power and the reactive power, this was been illustrated by the presence of the reactive power for a short moment at the step time.

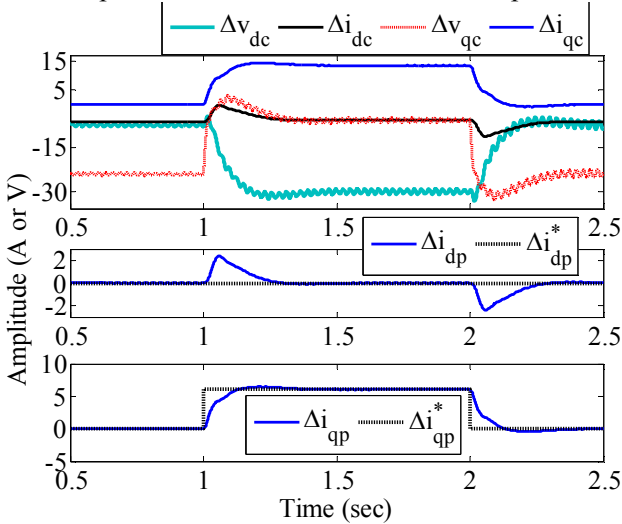


Fig. 13. Dynamic response when the rotor turns at rated speed with parameter uncertainties.

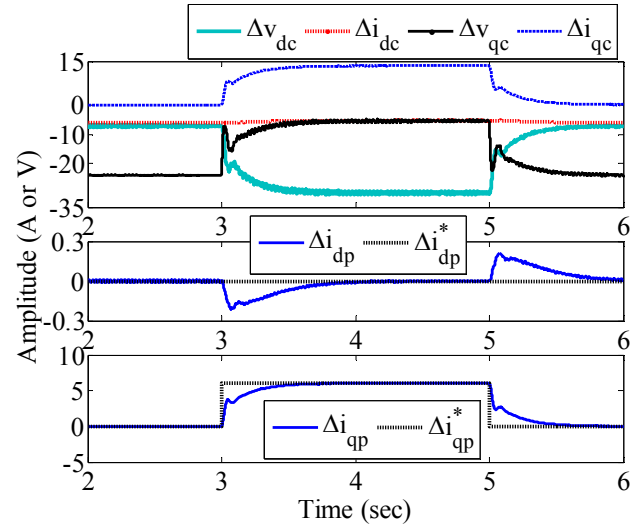


Fig. 14. Dynamic response when the rotor turns at 650 (rpm) with parameter uncertainties.

5. Conclusions

In this paper a mixed sensitivity H_∞ control of BDFIM as generator is performed. The wind energy system machine is considered connected directly to a balanced grid. This consideration allows us to develop a transfer function matrix model for the BDFIM, with the CW voltages as inputs, and the PW currents as outputs. Analytical studies indicate that the BDFIM is stable over all speed range. Besides that, small variations in the electric parameters of the BDFIM don't affect the stability, and therefore the BDFIM-stability is robust compared to temperature rising during the operation. To determine the suitable regulators of the produced power by the BDFIM, a decoupling method is applied and the controllers are calculated by the minimization of the H_∞ norm of the mixed sensitivity. To eliminate the steady state error, an integral action has been introduced by using the partial fraction technique. The simulation results of the proposed control scheme show that the controller can achieve fast response time, very good tracking and comfortable robustness margin in stability as well as in parameters uncertainties. Unfortunately, the more the parameters are imprecise the more the decoupling matrix has a weak effect.

References

1. Roberts, P. C., Long, T., McMahon, R. A., Shao, S., Abdi, E., & Maciejowski, J. M.: *Dynamic modelling of the brushless doubly fed machine*. In: IET Electric Power Applications, Vol. 7, No. 7, 2013, pp. 544-556.
2. Hunt, L. J.: *A new type of induction motor*. In: Journal of the Institution of Electrical Engineers, Vol. 39, No. 186, 1907, pp. 648-667.

3. Broadway, A. R. W., & Burbridge, L.: *Self-cascaded machine: a low-speed motor or high-frequency brushless alternator*. In: Proceedings of the Institution of Electrical Engineers, Vol. 117, No. 7, 1970, pp. 1277-1290.
4. Blazquez, F., Veganzones, C., Ramirez, D., & Platero, C.: *Characterization of the rotor magnetic field in a brushless doubly-fed induction machine*. In: IEEE Transactions on Energy Conversion, Vol. 24, No. 3, 2009, pp. 599-607.
5. Bouzekri, H., Ganouche, A., & Ahmida, Z.: *Investigation into control performance of Brushless Doubly Fed asynchronous machines in wind energy conversion systems*. In: 15th IEEE International Conference on Environment and Electrical Engineering, IEEEIC 2015, June, 2015, pp. 1099-1103.
6. Williamson, S., Ferreira, A. C., & Wallace, A. K.: *Generalised theory of the brushless doubly-fed machine. Part I. Analysis*. In: IEE Proceedings-Electric Power Applications, Vol. 144, No 2, 1997, pp. 111-122.
7. Poza Lobo, F. J.: *Modélisation, conception et commande d'une machine asynchrone sans balais doublement alimentée pour la génération à vitesse variable*. PhD Thesis, INPG, 2003, Grenoble.
8. Poza, J., Oyarbide, E., Roye, D., & Rodriguez, M.: *Unified reference frame dq model of the brushless doubly fed machine*. In: IEE Proceedings-Electric Power Applications, Vol. 153, No. 5, 2006, pp. 726-734.
9. Serhoud, H., & Benattous, D.: *Sensorless optimal power control of brushless doubly-fed machine in wind power generator based on extended kalman filter*. In: International Journal of System Assurance Engineering and Management, Vol. 4, No. 1, 2013, pp. 57-66.
10. Serhoud, H., & Benattous, D.: *Sliding mode control of brushless doubly-fed machine used in wind energy conversion system*. In: Revue des Energies Renouvelables, Vol. 15, No. 2, 2012, pp. 305-320.
11. Mahboub, M. A., Drid, S., Sid, M. A., & Cheikh, R.: *Sliding mode control of grid connected brushless doubly fed induction generator driven by wind turbine in variable speed*. In: International Journal of System Assurance Engineering and Management, 2016.
12. Wang, X., Yang, J., Zhang, X., & Wu, J.: *Sliding mode control of active and reactive power for brushless doubly-fed machine*. In: International Colloquium on Computing, Communication, Control, and Management, 2008 ISECS, Vol. 2, August, 2008, pp. 294-298.
13. Madbouly, S. O., Soliman, H. F., Hasanien, H. M., & Badr, M. A.: *Fuzzy logic control of brushless doubly fed induction generator*. In: 5th IET International Conference on Power Electronics, Machines and Drives, PEMD 2010, April, 2010, pp. 1-7.
14. Shao, Z., & Zhan, Y.: *Adaptive Fuzzy Sliding Mode Control for Brushless Doubly Fed Machine*. In: Second International Symposium on Computational Intelligence and Design, ISCID'09, Vol. 2, December, 2009, pp. 73-77.
15. Zhang, F., Jin, S., Pan, G., & Liu, G.: *Research on H_∞ mixed sensitivity control of brushless doubly-fed motor*. In: International Conference on Electrical Machines and Systems, ICEMS 2008, October, 2008, pp. 1531-1534.
16. Zhang, F., Jin, S., & Wang, X.: *L2 robust control for brushless doubly-fed wind power generator*. In: 2009 IEEE International Conference on Automation and Logistics, August, 2009, pp. 1335-1339.
17. Poza, J., Oyarbide, E., Sarasola, I., & Rodriguez, M.: *Vector control design and experimental evaluation for the brushless doubly fed machine*. In: IET Electric Power Applications, Vol. 3, No. 4, 2009, pp. 247-256.
18. Cook, C. D., & Smith, B. H.: *Stability and stabilisation of doubly-fed single-frame cascade induction machines*. In: Proceedings of the Institution of Electrical Engineers, Vol. 126, No. 11, 1979, pp. 1168-1174.
19. Cook, C. D., & Smith, B. H.: *Effects of machine parameter values on dynamic response and stability regions of doubly-fed cascade induction machines*. In: IEE Proceedings B-Electric Power Applications, Vol. 130, No. 2, March, 1983, pp. 137-142.
20. Li, R., Wallace, A., & Spee, R.: *Determination of converter control algorithms for brushless doubly-fed induction motor drives using Floquet and Lyapunov techniques*. In: IEEE transactions on power electronics, Vol. 10, No. 1, 1995, pp. 78-85.
21. Poza, J., Oyarbide, E., Roye, D., & Sarasola, I.: *Stability analysis of a BDFM under open-loop voltage control*. In: European Conference on Power Electronics and Applications, September, 2005.
22. Sarasola, I., Poza, J., Oyarbide, E., & Rodríguez, M. Á.: *Stability analysis of a brushless doubly-fed machine under closed loop scalar current control*. In: IECON 2006-32nd Annual Conference on IEEE Industrial Electronics, November, 2006, pp. 1527-1532.
23. Agbaje, O., Kavanagh, D. F., Sumislawska, M., Howey, D. A., McCulloch, M. D., & Burnham, K. J.: *Estimation of temperature dependent equivalent circuit parameters for traction-based electric machines*. In: Hybrid and Electric Vehicles Conference 2013, HEVC 2013, November, 2013, pp. 1-6.
24. Sumislawska, M., Agbaje, O., Kavanagh, D. F., & Burnham, K. J.: *Equivalent circuit model estimation of induction machines under elevated temperature conditions*. In: International Conference on Control, 2014 UKACC, July, 2014, pp. 413-418.
25. Sumislawska, M., Gyftakis, K. N., Kavanagh, D. F., McCulloch, M., Burnham, K. J., & Howey, D. A.: *The Impact of Thermal Degradation on Properties of Electrical Machine Winding Insulation Material*. In: IEEE Transactions on Industry Applications, Vol. 52, No. 4, 2016, pp. 2951-2960.
26. Ganouche, A., Bouzekri, H., & Beddar, A.: *Robust control of brushless doubly fed induction generator*. In: International Conference on Technological Advances in Electrical Engineering, ICTAEE'16, Skikda, October, 2016.
27. Zames, G.: *Feedback and optimal sensitivity: Model reference transformations, multiplicative seminorms, and approximate inverses*. In: IEEE Transactions on

- automatic control, Vol. 26, No. 2, 1981, pp. 301-320.
28. Doyle, J. C., Glover, K., Khargonekar, P. P., & Francis, B. A.: *State-space solutions to standard H_2 and H_∞ control problems*. In: IEEE Transactions on Automatic control, Vol. 34, No. 8, 1989, pp. 831-847.
 29. Doyle, J. C., Francis, B. A., & Tannenbaum, A. R.: *Feedback control theory*. Macmillan Publishing Company, New York, 1992.
 30. Gu, D. W., Petkov, H. P., & Konstantinov, M. M.: *Robust control design with MATLAB®*. Springer Science & Business Media, 2005.
 31. Verma, M., & Jonckheere, E.: *L_∞ -compensation with mixed sensitivity as a broadband matching problem*. In: Systems & control letters, Vol. 4, No 3, 1984, pp. 125-129.
 32. Kwakernaak, H.: *Minimax frequency domain performance and robustness optimization of linear feedback systems*. In: IEEE Transactions on Automatic Control, Vol. 30, No. 10, 1985, pp. 994-1004.
 33. Skogestad, S., & Postlethwaite, I.: *Multivariable feedback control: analysis and design*. Second Edition. New York: Wiley, 2001.
 34. Azimi, V., Nekoui, M. A., & Fakharian, A.: *Speed and torque control of induction motor by using robust H_∞ mixed-sensitivity problem via TS fuzzy model*. In: 20th Iranian Conference on Electrical Engineering, ICEE2012, May, 2012, pp. 957-962.
 35. Cárdenas, R., Peña, R., Wheeler, P., Clare, J., Muñoz, A., & Sureda, A.: *Control of a wind generation system based on a Brushless Doubly-Fed Induction Generator fed by a matrix converter*. In: Electric Power Systems Research, Vol. 103, 2013, pp. 49-60.